

# The Onset of Voltage Hash and its Relationship to Anode Spots in Magnetoplasmadynamic Thrusters

IEPC-2005-084

*Presented at the 29<sup>th</sup> International Electric Propulsion Conference, Princeton University  
October 31 – November 4, 2005*

Luke Uribarri\* and E. Y. Choueiri†

*Electric Propulsion and Plasma Dynamics Laboratory  
Department of Mechanical and Aerospace Engineering  
Princeton University, Princeton, New Jersey, 08544*

A phenomenological model is developed to elucidate the relationship between voltage hash and anode spots, which are two well-known invariant features of onset in magnetoplasmadynamic thrusters (MPDTs). As the total current in the thruster is increased (at a fixed mass flow rate) the enhanced radial electromagnetic force density leads to a mass depletion in the anode region which, in turn, leads to a disparity between the thermal current density to the anode and the current density imposed there by the circuit. An anode sheath voltage model that relates the sheath voltage to the charge density on the anode surface is derived for an anode experiencing a mass starvation crisis, and current continuity is used to relate the charge density to the transient contributions to current provided by anode spots. According to this model, rapid heating of irregularities on the anode results in the explosive release of a metal vapor plasma, whose contribution to the current collected at the anode drives down the sheath voltage. As the spot plasma dissipates, the voltage rises again; the repetition of this process is the origin of voltage hash. The order of magnitude (MHz) of the hash frequency predicted by the model for the expected physical parameters is consistent with observations.

## Nomenclature

$\alpha$	Thermal diffusivity, m <sup>2</sup> /s
$\alpha_s$	Ratio of temperatures $T_e/T_i$
$\bar{c}_s$	Average thermal velocity of species $s$ , m/s
$\dot{m}$	Mass flow rate, g/s
$\eta$	Normalized anode sheath voltage $V_a/T_e$
$\gamma$	Ratio of specific heats
$\Gamma_s$	Random thermal flux of particle $s$ , m <sup>-2</sup>
$\gamma_s$	Ratio of random to directed electron energy at sheath edge
$\lambda_D$	The Debye length, m
$\phi_a$	Anode metal work function, V
$\sigma$	Surface charge density, C/m <sup>2</sup>
$J$	Total circuit current, A
$j_a$	Current density at the anode surface, A/m <sup>2</sup>
$J_d$	Displacement current at the anode, A
$J_{th}$	Random thermal electron current, A
$j_{th}$	Random thermal electron current density, A/m <sup>2</sup>
$k$	Thermal conductivity, W/m-K
$k_B$	The Boltzmann constant, $1.38 \times 10^{-23}$ J/K

\*Graduate Student, Princeton University, uribarri@princeton.edu

†Chief Scientist EPPDyL, Associate Professor Mechanical and Aerospace Engineering Department, choueiri@princeton.edu

$m_s$	Atomic mass of species $s$ , kg
$m_{sp}$	Atomic mass of material in a spot, kg
$n_s$	Number density of species $s$ , $\text{m}^{-3}$
$q$	Fundamental charge, $1.602 \times 10^{-19}$ C
$r_o$	Initial spot radius, m
$T_e$	Electron temperature, eV
$T_s$	Temperature of species $s$ , eV
$T_{sp}$	Temperature of spot material, K
$u_p$	Spot expansion speed, m/s
$V_a$	Anode sheath voltage, V

## I. Introduction

BOTH theoretically and experimentally, it has long been known<sup>3,7</sup> that the both the exit velocity  $u_e$  and the efficiency of a magnetoplasmadynamic thruster (MPDT) increase monotonically with the ratio of the thruster current squared to the mass flow rate,  $J^2/\dot{m}$ . It has been equally long known that increasing this ratio above a limiting value leads to a crisis (“onset”) manifested by oscillations (“hash”) in the terminal voltage and spot damage on the anode. This anode damage places a limit on the thruster lifetime that must be surmounted if the MPDT is to become useful as a primary propulsion system.

Many researchers have offered possible explanations for the physical mechanism behind onset: an excessively large back-EMF in the flowing plasma;<sup>6</sup> run-away Joule heating;<sup>11</sup> and the excitation of plasma instabilities.<sup>12</sup> However, none of these theories provide a direct link between the voltage hash and the anode damage, both of which are invariant features of onset. In the present work we attempt to provide this link and demonstrate whether a prediction of the hash characteristics agrees with experimental observations.

We state the hash-spot link in terms of fluctuations in the magnitude of the anode sheath voltage under conditions of current-carrier starvation. We derive an expression for the electron-attracting anode sheath voltage in terms of the electric field at the anode surface, and then show how this electric field is affected by the transient appearance of metal vapor plasma from an anode spot.

Sections II.A, II.B, and II.C motivate the discussion of the anode sheath and spotting models. Sections II.D and II.E respectively present the derivation of the anode sheath model and of the influence of anode spot plasma on the sheath voltage. In section III we discuss the results of this model and compare to experimental observations.

## II. Phenomenological Model

MPDTs in the laboratory are operated at a fixed current level, with the terminal voltage free to float to wherever the dynamics of the thruster arc dictate. The oscillations in the thruster voltage trace above onset (Fig. 1) are indicative of rapidly varying thruster arc dynamics that are absent below onset (Fig. 2). This section will first argue that the voltage hash is caused by the formation and collapse of an anode sheath voltage under the action of anode spots, and then describe a phenomenological model to demonstrate how this can happen.

### A. The Importance of Anode Spots

There are several reasons to believe that the voltage hash corresponds to the action of spots on the surface of the anode. Anode spots—so called because they appear as small, short lived luminous points, or “spots,” on the anode surface—were associated with voltage hash in high-current vacuum arcs by Harris<sup>2</sup> in 1982. He observed that during a current pulse through his vacuum arc, hash in the voltage trace appeared at the same time as short-lived flashes of luminosity at the anode, and that the time scales of the two phenomena were similar. Vainberg et al.<sup>14</sup> similarly noted that the existence of voltage hash in their steady-state MPDT was associated with the appearance of spots on the anode, though they were less specific about how they observed such spots. The observations of these researchers, a small sampling of a larger body of such observations in the literature, encourage phenomenological modelling of voltage hash and anode spots.

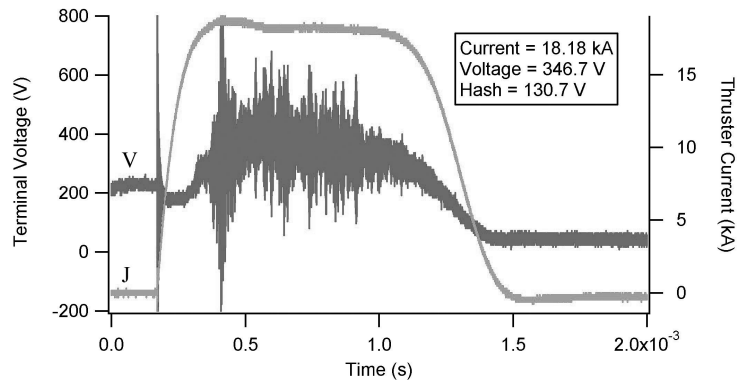


Figure 1. Typical voltage (V) and current (J) traces at an operating condition above onset for the Princeton FSBT,<sup>16</sup> operating with  $\dot{m} = 6$  g/s argon at 18 kA.

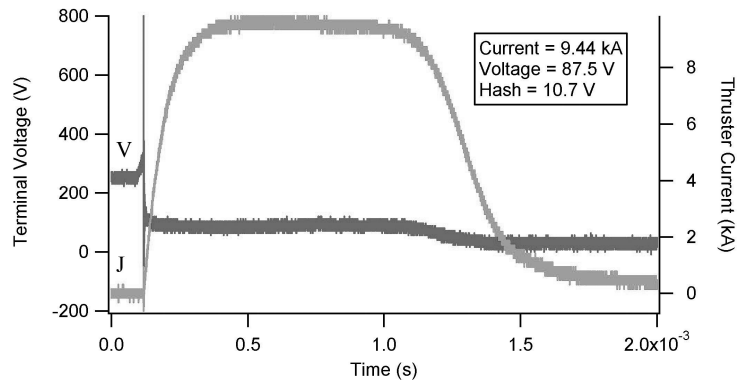


Figure 2. Typical voltage (V) and current (J) traces at an operating condition below onset for the Princeton FSBT,<sup>16</sup> operating with  $\dot{m} = 6$  g/s argon at 9 kA.

## B. Anode Starvation

A common premise behind much thinking about onset is the idea that the anode is being starved of its ability to collect sufficient current from the plasma, a consequence of the  $\mathbf{j} \times \mathbf{B}$  force component that forces plasma toward the centerline of the thruster's axial geometry<sup>5,10</sup>—away from the anode. Oberth and Jahn<sup>10</sup> concluded that at conditions for which the MPDT was “overfed”—i.e., for which  $J^2/\dot{m}$  is small—the current conduction to the anode was accomplished by a random thermal flux of electrons; by contrast, when the MPDT was “underfed”— $J^2/\dot{m}$  large—substantial electric fields were required to make up for an electron density too small to fully conduct the current by random thermal flux. Diamant<sup>1</sup> extended this idea to his discussions of anode spotting by showing that the appearance of anode spots corresponds to the condition in which the actual current density at the anode was greater than the plasma could supply from thermal electrons. Oberth and Jahn observed the importance of this condition: the electric fields that accompany underfed conditions increase the energy of electrons that reach the anode surface, so that the anode is subjected to ever larger heat fluxes as conditions become more underfed. It is likely that these heat fluxes are related to the formation of anode spots.

## C. Anode Heat Flux

The energy deposition on the anode per unit area per unit time is the sum of the incident electrons' thermal energy, their directed energy attained by falling through an anode sheath, and the energy released as they “condense” into the anode metal:<sup>10</sup>

$$\dot{q} = j_a \left( \frac{5}{2} T_e + V_a + \phi_a \right) \quad (1)$$

where  $j_a$  is the current density,  $T_e$  the electron temperature in eV,  $V_a$  the anode sheath voltage, and  $\phi_a$  the anode metal work function. Using this relationship to calculate anode heating requires an expression for  $V_a$ .

## D. The Anode Sheath

Vainberg et al.<sup>14</sup> and Klyarfel'd et al.<sup>4</sup> have previously shown experimentally that the anode sheath potential in a high-current arc is negative (electron-repelling) at low currents but transitions to positive values as the current in the arc is increased. Vainberg et al., with Oberth and Jahn, and Diamant, suggested that this transition occurs when the total thruster current exceeds that which the anode passively collects from thermal electrons in the plasma.

The thermal electron current collected by the anode,  $J_{th}$ , derives from the random thermal electron current density,  $j_{th}$ , integrated over the area of the anode  $A_a$ .  $j_{th}$  in turn arises due to the mass disparity between electrons and ions: at the plane of the anode, the flux  $\Gamma_s$  of either species  $s$  onto the surface is

$$\Gamma_s = \frac{n_s \bar{c}_s}{4} = \frac{n_s}{4} \left( \frac{8qT_s}{\pi m_s} \right)^{1/2}, \quad (2)$$

where  $n_s$ ,  $T_s$ ,  $m_s$ , and  $\bar{c}_s$  are the number density, temperature (in eV), atomic mass, and average thermal velocity of species  $s$ , and  $q$  is the fundamental charge. When the plasma is quasineutral and consists of only one species of ions and electrons, the ratio of their fluxes is

$$\frac{\Gamma_e}{\Gamma_i} = \left( \frac{T_e}{T_i} \right)^{1/2} \left( \frac{m_i}{m_e} \right)^{1/2} \approx 10^3 \quad (3)$$

where the numerical approximation is for an argon plasma with  $T_e = T_i$ . Because the flux of electrons dominates, the anode sees

$$j_{th} = q\Gamma_e = \frac{n_e q}{4} \left( \frac{8qT_e}{\pi m_e} \right)^{1/2}, \quad (4)$$

so that the current passively collected at the anode is

$$J_{th} = \int_S j_{th} dA_a. \quad (5)$$

The current continuity equation at the anode is

$$J_c = J_{th} + J_d, \quad (6)$$

where  $J_c$  is the current demanded by the external circuit and  $J_d$  is the displacement current, defined by this equation, which represents the accumulation of charge on the anode when  $J_c \neq J_{th}$  (see Fig. 3). Considering the anode metal as a perfect conductor, the charge accumulation of  $J_d$  must occur on the anode surface so that the surface charge density  $\sigma$  changes in time according to

$$\frac{d\sigma}{dt} = \frac{J_d}{A_a} = \frac{J_c - J_{th}}{A_a}. \quad (7)$$

Gauss' Law states that the electric field at the surface of a conductor is a function of the charge density there:

$$E_o = \frac{\sigma}{\epsilon_o}. \quad (8)$$

This electric field value can be used as one boundary condition for a sheath voltage calculation; and since the change in this electric field in time is known (via Eqs. (7) and (8)), the resulting expression for the sheath voltage will provide insight into how the sheath voltage changes in time.

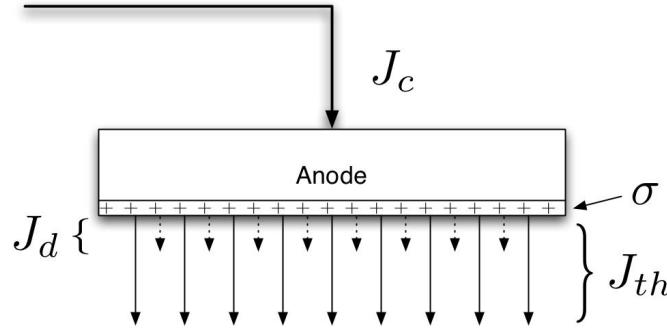


**Figure 3.** The anode as a current conduit, showing the current demanded by the power supply circuit ( $J_c$ ), the current supplied by the plasma ( $J_{th}$ ), and the displacement current ( $J_d$ ) representing the charging of the anode surface ( $\sigma$ ). Arrows not to scale;  $J_d \ll J_{th}$ .

The rest of the sheath calculation is predicated on three assumptions, justification for which appear in Diamant's<sup>1</sup> data: first, the sheath is unmagnetized and collisionless (its thickness, on the order of the Debye length  $\lambda_D = \sqrt{\epsilon_o T_e / q n_e}$ , is smaller than the electron gyroradius and mean free path); second, the sheath voltage is a positive value (electron-attracting and ion-repelling) large enough that the incoming electrons can be considered monoenergetic (i.e., that  $V_a > T_e$ ). Under these conditions, the sheath voltage is given by the solution of the following set of coupled equations: the Poisson equation,

$$\nabla^2 V_a(\mathbf{r}) = -\frac{q}{\epsilon_o} (n_i(\mathbf{r}) - n_e(\mathbf{r})); \quad (9)$$

the electron continuity and energy equations,

$$n_{e,\infty} u_{e,\infty} = n_e(\mathbf{r}) u_e(\mathbf{r}) \quad (10)$$

$$m_e u_e(\mathbf{r})^2 = m_e u_{e,\infty}^2 + 2q V_a(\mathbf{r}); \quad (11)$$

and a Boltzmann distribution of ions throughout the sheath

$$n_i(\mathbf{r}) = n_{i,\infty} e^{-V_a(\mathbf{r})/T_i}. \quad (12)$$

$u_e(\mathbf{r})$  is the electron velocity at position  $\mathbf{r}$  in the sheath, and the subscript  $\infty$  refers to positions far from the anode. Solving Eq. (10) for the electron density  $n_e(\mathbf{r})$  and inserting both this and  $n_i(\mathbf{r})$  from Eq. (12) into Eq. (9),

$$\nabla^2 V_a(\mathbf{r}) = -\frac{qn}{\epsilon_o} \left[ e^{-V_a(\mathbf{r})/T_i} - \left( 1 + \frac{2qV_a(\mathbf{r})}{m_e u_{e,\infty}^2} \right)^{-1/2} \right]. \quad (13)$$

Quasineutrality was invoked outside the sheath, letting  $n_{e,\infty} = n_{i,\infty} = n$ . This equation can be conveniently normalized by the following substitutions:

$$\alpha_s = \frac{T_e}{T_i} \quad (14)$$

$$\eta = \frac{V_a}{T_e} \quad (15)$$

$$\gamma_s = \frac{2qT_e}{m_e u_{e,\infty}^2} \quad (16)$$

$$\nabla_n = \lambda_D \nabla \quad (17)$$

to produce

$$\nabla_n^2 \eta = (1 + \gamma \eta)^{-1/2} - e^{-\alpha \eta}. \quad (18)$$

The boundary conditions on this equation include the already-mentioned electric field at the anode surface, and the values of the potential and electric field outside the sheath, both of which are set to zero:

$$\nabla_n \eta|_o = -\frac{\sigma \lambda_D}{\epsilon_o T_e} \quad (19)$$

$$\nabla_n \eta|_\infty = 0 \quad (20)$$

$$\eta(\infty) = 0. \quad (21)$$

Solutions to this equation with these boundary conditions provide values for the anode sheath potential as a function of  $\sigma$ , which in turn is a function of time while anode spot action is occurring. This sheath equation, then, provides the link between anode spotting and oscillations in the anode sheath potential.

Only in one dimension does the solution to Eq. (18) have an analytical form, which is transcendental in  $\eta_o$ , the value of the potential at the anode surface:

$$\frac{1}{\alpha} e^{-\alpha \eta_o} + \frac{2}{\gamma} \sqrt{1 + \gamma \eta_o} = \frac{2}{\gamma} + \frac{1}{\alpha} + \frac{1}{2} \left( \frac{\lambda_D \sigma}{\epsilon_o T_e} \right)^2. \quad (22)$$

## E. Spot Formation and Current

The simplest way to consider the formation of a spot is as the explosive release of a certain amount of material from the anode surface. The energy input from the plasma electrons, given by Eq. (1), heats the anode rapidly to a temperature at which a significant density of metal atoms are vaporized, and this metal vapor is explosively released from the surface. The melting temperature of the metal is a sufficient temperature for this to happen; in the vacuum conditions in which the MPDT is operated, the boiling temperature is reduced to values close to the melting temperature,<sup>13</sup> and once the metal has been melted, the pressure of the incoming electrons will help to drive the molten metal to atomization. The ionization of the metal vapor happens quickly compared to the time necessary for the vapor to expand significantly, and for practical purposes may be considered instantaneous.

The presence of a spot at the anode surface enhances the current density there, given by Eq. (4), due to the higher plasma density in the spot compared to that in the ambient plasma. The spot plasma can make only a transient appearance, however, because it will quickly expand into the background until its density has dropped to that of the ambient plasma. A zeroth-order approximation employed in the field of laser ablation<sup>9</sup> considers the spot to expand spherically, with spatially uniform density, and a front expansion speed

$$u_p = \sqrt{\frac{2}{\gamma - 1}} \sqrt{\frac{\gamma k_B T_{sp}}{m_{sp}}}, \quad (23)$$

where  $\gamma$  is the ratio of specific heats,  $T_{sp}$  is the temperature of the expanding material,  $m_{sp}$  is the atomic mass of the spot material, and  $k_B$  the Boltzmann constant.

A spot expanding in this manner contains a density that drops like the cube of the time since the beginning of its expansion

$$\frac{n(t)}{n_o} = \left( 1 + \frac{u_p t}{r_o} \right)^{-3}, \quad (24)$$

where  $r_o$  is the radius of the spot when it first forms. During the expansion, the spot density contributes to the current collected by the anode an additional current of magnitude

$$J_{sp} = \pi(r_o + u_p t)^2 q n_o \left(1 + \frac{u_p t}{r_o}\right)^{-3} = \frac{\pi r_o^2 q n_o}{1 + \frac{u_p t}{r_o}} \quad (25)$$

and in doing so alters the balance of currents that determines the charge density  $\sigma$  on the anode—and, by Eq. (22), the anode sheath potential. The additional current collected through the spot will drive down the sheath potential, until the spot has diffused into the background; then the sheath potential will rise again, until the formation of another spot.

## F. Heating at the Anode Surface

The reason for the appearance of damage at a spot, instead of in a broader area, is anode irregularity. Even a polished metal surface has a rough microstructure that gives rise to points of preferential electric field enhancement and heating.<sup>8</sup> The scale of this roughness is on the order of a few to tens of microns.<sup>15</sup> Because of this smallness of scale, the heat penetration length  $\sqrt{\alpha t}$  usually exceeds the dimension of the microstructure and the heating of the irregularity follows a lumped-heat-capacity model:

$$\frac{\partial T}{\partial t} = \frac{2\dot{q}\alpha}{kr}. \quad (26)$$

Here  $\alpha$  is the thermal diffusivity and  $k$  the thermal conductivity of the anode material, and  $r$  is the scale length of the irregularity.

The typical electric field enhancement factor  $\beta$  for a polished cathode that has been subjected to some arcing is  $\beta \sim 20$ .<sup>8</sup> In the absence of similar knowledge about anode irregularities, we will take this to be typical for our anode as well. An enhanced electric field at an irregularity translates to an enlarged sheath potential at that point, as governed by Eq. (18). The value of  $V_a$  contributing to the heating of the point will therefore in general be larger than the gross value of  $V_a$  for the anode as a whole. The factor by which  $V_a$  is amplified at an irregularity can be calculated from Eq. (18).

## III. Results

In this section, the model of the last section will be used to calculate the frequency and magnitude of oscillations in the anode sheath voltage, which will then be compared to observations of the same quantities in the Princeton FSBT.

Eqs. (22), (7), (1), (25), and (26) provide sufficient information to show the oscillatory behavior of an anode subjected both to starvation ( $J_c > J_{th}$ ) and to anode spots. These equations were integrated forward in time using the following scheme.

- The temperature of an irregularity of a given size  $r_o$  is observed under a heat flux  $\dot{q}$  until it reaches the material melting temperature  $T_m$ .
- When  $T_m$  is reached, a spot mass is released, and its density under expansion is watched. Its contribution to the current is calculated.
- The surface charge density is continually updated during each phase as it changes according to Eq. (7), where now  $J_{th}$  includes any contribution from a spot.
- The sheath voltage is calculated from the surface charge density. It decreases when a spot is released and increases when there is no spot.

The material properties of copper were used for these calculations. The electron density in the spot before expansion was taken to be  $2 \times 10^{27} \text{ m}^{-3}$ , which corresponds to an ionization fraction of 0.1 in a spot of density equal to that of molten copper. The background density of electrons and their temperature were chosen to be  $n_e = 1 \times 10^{19} \text{ m}^{-3}$  and  $T_e = 3 \text{ eV}$ , orders of magnitude that have justification in the data of Diamant.<sup>1</sup> The size of the irregularity and initial spot radius were set to  $r_o = 10 \text{ }\mu\text{m}$ , which we found to be

the order of magnitude of “pristine” spots (i.e., that showed no evidence of multiple overlapping spots) on the anodes of the FSBT.

We have no data specific to the anodes on the FSBT for the field enhancement factor  $\beta$ . On one extreme, the anode can be considered perfectly flat with no irregularities, so that  $\beta = 1$ . Researchers have found values of  $\beta$  ranging into the hundreds, but for our purposes we will take the figure cited in the last section,  $\beta \sim 20$ , as the other extreme.

One further parameter that must be specified arises from Eq. (7):

$$\frac{d\sigma}{dt} = \frac{J_c - J_{th}}{A_a} = \frac{J_c - (J_{th,0} + J_{sp})}{A_a} = \frac{\Delta J - J_{sp}}{A_a}. \quad (27)$$

This parameter  $\Delta J$  is an indicator of how “starved” the anode is for charge carriers.  $J_{sp,0}$  is the thermal current provided to the anode in the absence of any spots. There is no data in MPDTs to indicate what the magnitude of  $\Delta J$  should be; however, we can make the following argument.

If the anode sheath is modelled as a parallel-plate capacitor, then the voltage across it is related to the charge by

$$V = \frac{Qd}{\epsilon_0 A_a}, \quad (28)$$

where  $Q$  is the charge on the capacitor and  $d$  is the separation between plates. The order of magnitude of the sheath width will be used for  $d$ , so  $d \sim 10\mu\text{m}$ . A voltage change  $\Delta V$  across the capacitor in time  $\Delta t$  occurs because of the displacement current  $\Delta Q/\Delta t = \Delta J$ :

$$\Delta J = \frac{\epsilon_0 A_a}{d} \frac{\Delta V}{\Delta t}. \quad (29)$$

If we let  $\Delta V = 200$  V and  $\Delta t = 7 \times 10^{-7}$  s, which are a typical amplitude and a typical timescale for the voltage hash, and  $A_a = 0.044$  m<sup>2</sup> (which is the FSBT anode area), then  $\Delta J \approx 10$  A. We therefore expect that the magnitude of  $\Delta J$  will be on this order.

The results of the computation indicate that for all of the above parameters, the frequency of the anode sheath oscillations is about 3 MHz. The value of  $\beta$  does not affect the frequency.  $\beta$  does affect the amplitude of the oscillations; for example, the above calculation was carried out with  $\beta = 6$  and produced an oscillation amplitude of about 400 V. This number decreases with increasing  $\beta$ .

The output of this computation can be matched with the experimentally observed frequency (1.3 MHz) and amplitude order (several hundred volts) by choosing  $\beta \sim 6$  and  $\Delta J = 5$  A. A plot of the computed oscillations is shown in Fig. 4. The sharp peaks exist on the oscillations because we have modelled the spot mass ejection as an instantaneous explosion, rather than as the more gradual release that probably happens in reality. For comparison, experimentally observed hash is shown in Fig. 5.

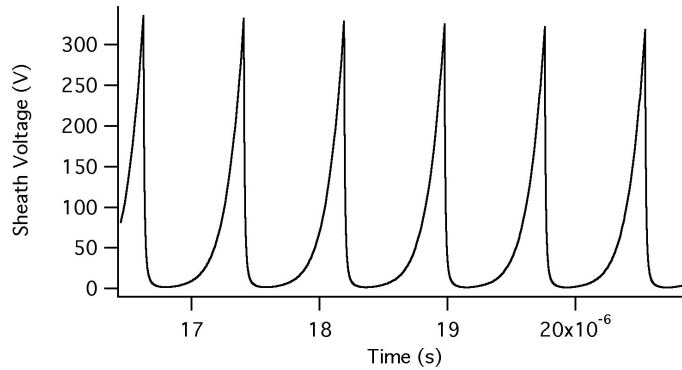


**Figure 4.** An example result of the sheath model.  $\beta = 6$ ,  $\Delta J = 5$  A.

One important insight gained from this model is that the computed frequency of the sheath voltage oscillations is determined by the amount of time that the spot current makes up for  $\Delta J$ . It is therefore the physics of the metal vapor plasma that sets the frequency here, rather than any dependence upon the thermal properties of the anode material.

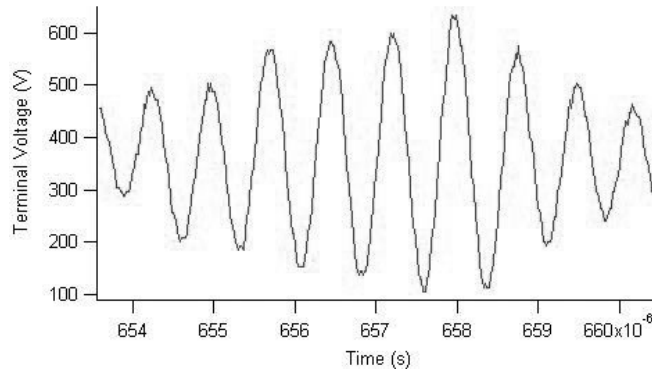


Figure 5. An expanded view of the voltage trace in Fig. 1, showing the amplitude and timescale of the voltage fluctuations.

## IV. Conclusion

In this paper, we have put forward a phenomenological model that seeks to explain the relationship between voltage hash and anode spot damage, the two invariant features of the onset phenomenon. To do this, we have developed a model for the anode sheath voltage that accepts the electric field at the anode surface as one boundary condition. We have used Gauss' Law to relate the electric field to the surface charge density on the anode, and we have related the time change of surface charge density to the appearance and disappearance of anode spot mass. The physical sequence of events that this models is: the anode sheath voltage increases in time as a result of the anode starvation; a small irregularity on the anode is heated due to this increasing voltage until it releases a significant quantity of metal vapor; this new source of plasma density enhances the current and reduces the anode starvation, forcing the sheath voltage to fall; and when the metal vapor density has dropped sufficiently due to expansion, the anode is again starved and the process repeats itself. We have postulated that this rise and fall of the anode sheath voltage is associated with voltage hash.

Computations using this model have shown that for typical values of the physical parameters, voltage oscillations have a frequency on the order of a few MHz (we computed the frequency to be about 3 MHz for the most typical parameters we expected), which agrees in order of magnitude with experimental observations. The prediction of frequency depends on the specific value of the anode starvation current  $\Delta J$  used, but not on the value of the electric field enhancement factor  $\beta$ .  $\beta$  does affect the prediction of the oscillation magnitude. Matching the experimental observations can be done by taking  $\Delta J = 5$  A and  $\beta \sim 6$ . Future modelling work will concentrate on creating accurate models to better predict these values for MPDTs.

## References

- <sup>1</sup>Kevin D. Diamant. *The Anode Fall in a High Power Pulsed MPD Thruster*. PhD thesis, Princeton University, 1996.
- <sup>2</sup>L.P. Harris. Small-scale anode activity in vacuum arcs. *IEEE Transactions on Plasma Science*, PS-10(3):173–180, September 1982.
- <sup>3</sup>Robert G. Jahn. *Physics of Electric Propulsion*. McGraw-Hill, 1968.
- <sup>4</sup>B.N. Klyarfel'd, N.A. Neretina, and N.N. Druzhinina. Anode Region in a Low-Pressure Gas Discharge: IV. Anode Phenomena in a High-Current Mercury Discharge (Survey). *Soviet Physics Technical Physics*, 17(6):997–1005, December 1972.
- <sup>5</sup>A.G. Korsun. Current limiting by self magnetic field in a plasma accelerator. *Soviet Physics Technical Physics*, 19(1):124–126, July 1974.
- <sup>6</sup>J.D. Lawless and V. V. Subramaniam. Theory of Onset in Magnetoplasmadynamic Thrusters. *Journal of Propulsion and Power*, 3(2):121–127, March/April 1987.
- <sup>7</sup>A.C. Malliaris, R.R. John, R.L. Garrison, and D.R. Libby. Performance of quasi-steady mpd thrusters at high powers. *AIAA Journal*, 10(2):121–122, February 1972.
- <sup>8</sup>Gennady A. Mesyats. *Cathode Phenomena in a Vacuum Discharge: The Breakdown, the Spark and the Arc*. Nauka, 2000.
- <sup>9</sup>John C. Miller and Richard F. Haglund Jr., editors. *Laser Ablation and Desorption*. San Diego: Academic Press, 1998.
- <sup>10</sup>R.C. Oberth and R.G. Jahn. Anode phenomena in high-current accelerators. *AIAA Journal*, 10(1):86–91, January 1972.
- <sup>11</sup>H.O. Schrade, Thomas Wegmann, and Thomas Rosgen. The onset phenomena explained by run-away joule heating. *Proceedings of IEPC-1991*, (22), 1991.

<sup>12</sup>A.P. Shubin. Dynamic nature of critical regimes in steady-state high-current plasma accelerators. *Soviet Journal of Plasma Physics*, 2(1):18–21, January/February 1976.

<sup>13</sup>American Welding Society. *Brazing Manual*. Miami: American Welding Society, 3rd edition, 1976.

<sup>14</sup>L.I. Vainberg, G.A. Lyubimov, and G.G. Smolin. High-current discharge effects and anode damage in an end-fire plasma accelerator. *Soviet Physics Technical Physics*, 23(4):439–443, April 1978.

<sup>15</sup>D.W. Williams and W.T. Williams. Prebreakdown and breakdown characteristics of stainless steel electrodes in vacuum. *Journal of Physics D: Applied Physics*, 7:1173–1183, 1974.

<sup>16</sup>J.K. Ziemer and E.Y. Choueiri. Quasi-steady magnetoplasmadynamic thruster performance database. *Journal of Propulsion and Power*, 17(4):520–529, Sept/Oct 2001.